Nonlinear effects in the emission and absorption spectra of gases in resonant optical fields

I. M. Beterov and R. I. Sokolovskiĭ
Institute of Semiconductor Physics, Siberian Division
USSR Academy of Sciences, Novosibirsk; Moscow Institute of Steel and Alloys
Usp. Fiz. Nauk **110**, 169-190 (June 1973)

The review systematizes the experimental material and reports the fundamental theoretical results on the study of nonlinear resonance effects in spectra of atomic systems situated in the radiation field of lasers. The theoretical part explains the topics of greatest importance and significance for understanding of the experimental studies: the Stark effect in an optical field; the nonequilibrium velocity distribution of the atoms; the shape of the spectral line for a transition adjacent to a transition combining with a strong field; the simultaneous manifestation of the Stark effect and of Doppler broadening in the form of a very sharp structure on the line contour; a brief mention of the influence of collisions, recoil, and other factors on the sharp structure in spectra. The experimental part reports the results of experiments on the observation of the Stark effect in the optical region of the spectrum, the fine structure of the profile of a Doppler-broadened line and its properties, namely the dependence on the observation direction, the anisotropy in the field of a standing wave, the polarization properties, etc. in spectra of spontaneous or stimulated emission, absorption, and generation.

CONTENTS

1. INTRODUCTION

The development of high-power coherent sources of light in the optical band has made it possible to observe many nonlinear phenomena in spectra of atomic systems. Interest in such phenomena had already been evinced in radiospectroscopy, where the Stark effect was investigated in high-power radio-frequency fields[1]. In the optical region of the spectrum, the shifts[2-4] and splitting[5] of atomic levels were observed relatively recently in the giant fields of solid-state lasers. This question is elucidated in sufficient detail in the review[4] and the monograph[6]. For direct observation of the Stark splitting, very strong optical fields were used, in which the magnitude of the splitting[5,7] greatly exceeded the line width. Under these conditions it can be assumed that the spectral lines are homogeneously broadened and the situation is fully equivalent to that obtaining in radiospectroscopy.

Gas-laser fields are, as a rule, weaker. The Stark shifts produced by them are comparable with the natural line width Γ and are much smaller in the optical band than the Doppler width $k\bar{v}$ ($\Gamma \ll k\bar{v}$) due to the thermal motion of the atoms. Allowance for the inhomogeneous broadening of the spectral lines assumes then fundamental importance. It is curious that the Stark effect is not masked by the motion of the atoms and becomes manifest quite uniquely in the emission and absorption spectra of the atoms.

One of the reasons for this is the onset of a nonequilibrium velocity distribution of the atoms in the field of a plane monochromatic wave. The latter can be represented as the sum (difference) of the Maxwellian and Bennett velocity distributions of the atoms[8,9]:

$$w_B(v) \sim (\pi^{1/2}\bar{v})^{-3} e^{-v^2/\bar{v}^2}\Gamma_B/\pi\,[(\omega - \omega_{mn} - \mathbf{kv})^2 + \Gamma_B^2], \qquad (1.1)$$

where ω and k are the frequency and the wave vector of the strong field, ω_{mn} is the frequency of the atomic transition that is at resonance with the field, $\bar{v} = (2kT/M)^{1/2}$, $\Gamma_B = \Gamma(1+\kappa)^{1/2}$, Γ is the natural line width, and κ is a saturation parameter[9]. The distribution (1.1), superimposed on a Maxwellian contour, is known in the literature as a Bennett dip (spike). The formation of the nonequilibrium distribution is the consequence of the effect of saturation in a strong field[10]. The saturation maximum is reached for atoms in which the deviation $\Omega = \omega - \omega_m$ of the field from the atomic resonance ω_{mn} is offset by the Doppler shift (see (1.1)). Thus, an effective atomic beam with the velocity distribution (1.1), which can conveniently be called a Bennett beam, appears in the field of a monochromatic wave.

The onset of the Bennett beam and its interaction with the strong field lead to the formation of the fine structure on the Doppler contour of the line. The characteristic parameters of the fine structure are determined by the relaxation constants of the combining levels. The observed nonlinear effects can be used to determine the optical parameters of matter, which are usually hidden by the Doppler broadening. It is now customary to classify this new group of optical phenomena as belonging to nonlinear spectroscopy, which makes it possible to measure, relatively simply and with unusually high accuracy, material characteristics that cannot be determined by linear spectroscopy. The same phenomena are connected also with such questions of practical importance as the development of optical frequency standards and frequency conversion in the optical band.

The simplest situation occurs in the investigation of the emission or absorption spectrum in a transition that

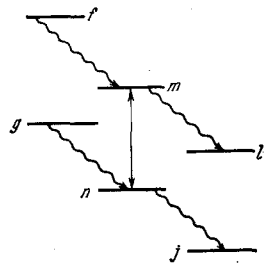

FIG. 1. Scheme of considered transitions.

is adjacent to a transition that combines with a strong field. The possible transitions are shown in Fig. 1 by wavy lines. It is precisely this case which has become the subject of many experimental and theoretical investigations.

In the present article we attempt to systematize experimental material and describe the principal results of the theory of nonlinear effects in a three-level system. In Chap. 2 we consider the theory of the fine structure of a Doppler-broadened spectral line in an external electromagnetic field constituting a plane monochromatic wave. Chapter 3 reports the results of experiments in the observation of the fine structure of the profile of a Doppler-broadened line in the spectra of spontaneous and stimulated emission and absorption.

2. THEORY OF FINE STRUCTURE OF DOPPLER-BROADENED SPECTRAL LINE IN AN EXTERNAL ELECTROMAGNETIC FIELD

When resonant nonlinear phenomena in atomic spectra of gaseous systems are considered, one can start from two points of view, one based on the terms of the unperturbed atom and the other on the energy levels of the atom-plus-field system. In the former case, the observed nonlinear phenomena are interpreted as multiphoton transitions[11] between the energy levels of the unperturbed atoms. In the latter case the analysis is based on single-photon transitions between energy levels of the system consisting of the atom and a strong field. The second approach is not restricted to perturbation theory in terms of the energy of the interaction of the atom with the strong field, and will be used in present paper.

The interpretation of the resonant phenomena is based on the theory of the Stark effect in the electromagnetic-wave field[1-5,12]. We consider the Schrödinger equation for an atom in a classical field with allowance for spontaneous relaxation described by an operator $\hat{\gamma}$ [13,15]:

$$i\hbar\,[(\partial/\partial t + \hat{\gamma})]\,\Psi = (\mathscr{H}_0 - \mathbf{DE})\,\Psi; \qquad (2.1)$$

Here $\mathscr{H}_0$ is the Hamiltonian of the atom, **D** is the dipole-moment operator, and **E** is the intensity of the electromagnetic field. In the energy representation, the operator $\hat{\gamma}$ is diagonal, with $\langle n|\hat{\gamma}|n\rangle = \gamma_n/2$, where γ_n is the natural width of the level. It is assumed that all the frequencies of the atomic transitions are different.

We replace the atomic system in an electromagnetic field consisting of two plane monochromatic waves with frequencies ω_0 and ω_μ, the wave vectors of which are parallel,

$$\mathbf{E}(t, \mathbf{r}) = \mathbf{E}_0 \cos(\omega_0 t - \mathbf{kr}) + \mathbf{E}_\mu \cos(\omega_\mu t - \mathbf{k}_\mu \mathbf{r}). \qquad (2.2)$$

We assume that the field with frequency ω_0 is resonant to the m – n transition between two excited states, and that its intensity is sufficient for nonlinear effects to become manifest. The field with frequency ω_μ is resonant to one of the adjacent transitions shown in Fig. 1 by wavy lines. We choose the latter transition to be, for example, g – n. The field intensity $\mathbf{E}_\mu$ is assumed to be weak enough for neglect of the nonlinear effects and use of only the first order of perturbation theory in the calculations.

In the resonant approximation it is easy to obtain from (2.1), in the Dirac representation[16], a system of equations relating the probability amplitudes C_m, C_n, and C_g of finding the atom in the states m, n, and g, respectively:

$$\left.\begin{aligned} dC_m/dt &= -(\gamma_m/2)\,C_m - iVe^{-i\Omega t}C_n, \\ dC_n/dt &= -(\gamma_n/2)\,C_n - iV^* e^{i\Omega t}C_m - iV_\mu^* e^{i\Omega_\mu t}C_g, \\ dC_g/dt &= -(\gamma_g/2)\,C_g - iV_\mu e^{-i\Omega_\mu t}C_n; \end{aligned}\right\} \qquad (2.3)$$

Here

$$V = -\mathbf{D}^{mn}\mathbf{E}_0/2\hbar,\ V_\mu = -\mathbf{D}^{gn}\mathbf{E}_\mu/2\hbar,\ \Omega = \omega_0 - \omega_{mn},\ \Omega_\mu = \omega_\mu - \omega_{gn},$$

$\mathbf{D}^{mn}$ and $\mathbf{D}^{gn}$ are the matrix elements of the dipole moment of the transitions m – n and g – n, respectively.

We assume that the atom was excited at the initial instant t_0 to one of the considered levels. The energy absorbed (emitted) by the atom per unit time at the frequency ω_μ is equal to the average value of the operator $e\mathbf{v}\mathbf{E}$. In the resonant approximation we have

$$d\mathscr{E}/dt = -2\hbar\omega_\mu \operatorname{Re}(iV_\mu e^{-i\Omega_\mu t}C_n C_g^*). \qquad (2.4)$$

If the atom landed on the level g, we can assume that at an instant of time $t > t_0$

$$C_g(t) = e^{-\gamma_g(t-t_0)/2}, \qquad (2.5)$$

and the calculation of the energy lost by the atom per unit time reduces to a solution of the first two equations of system (2.3). At $V_\mu = 0$, these equations describe the time variation of the atomic amplitudes of a two-level system in a harmonic field. The solution of such a problem is well known[9,12]. Under the influence of a strong field, the atomic system executes transitions between the levels m and n. As a result, the amplitudes C_n experience harmonic oscillations with frequencies

$$\Omega_{1,2} = -\{\Omega + i\Gamma \mp [(\Omega - i\gamma)^2 + 4|V|^2]^{1/2}\}/2, \qquad (2.6)$$

where $\Gamma = (\gamma_m + \gamma_n)/2$ and $\gamma = (\gamma_n - \gamma_m)/2$.

When $V_\mu \neq 0$, the right-hand side of the equations acquires a term describing the excitation of the state n in the radiative transition from the state g, with emission of a quantum $\hbar\omega_\mu$. The maximum value of C_n and the corresponding maximum value of the radiated energy (2.4) are attained when $-\Omega_\mu$ is at resonance with one of the frequencies $\Omega_{1,2}$. The spectroscopic interpretation of this phenomenon is exceedingly lucid. The interaction leads to splitting of the atom-plus-strong-field system into two sublevels (the Stark effect in a resonant field[1,4]) with energies

$$E_n + \hbar\Omega_1, \quad E_n + \hbar\Omega_2. \qquad (2.7)$$

The resonances correspond to the frequencies $(E_g - E_n - \hbar\Omega_n)/\hbar$ and $(E_g - E_n - \hbar\Omega_2)/\hbar$ of the transitions shown by the wavy lines in Fig. 2.

The foregoing is seen directly from the expression for the average radiation power of an ensemble of atoms at a time-constant pumping Q_g of the atoms to the level g:

$$\frac{d\bar{\mathscr{E}}}{dt} = 2\hbar\omega_\mu |V_\mu|^2 N_g \operatorname{Re}\left[\frac{(\gamma_m/2) - i(\Omega + \Omega_1)}{\Omega_2 - \Omega_1}\,\frac{1}{\Omega_\mu + \Omega_1 - i(\gamma_g/2)} + (1 \leftrightarrow 2)\right]; \qquad (2.8)$$

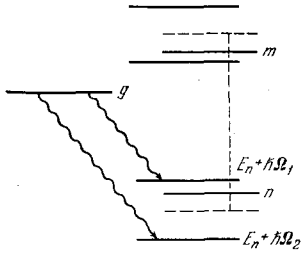

FIG. 2. Structure of terms in a strong monochromatic field.

here $N_g = Q_g/\gamma_g$; the parentheses $(1 \leftrightarrow 2)$ denote that the second term in (2.8) is obtained from the first by replacing the indices 1 by 2, and vice versa.

The splitting (2.7), (2.8) was first observed in the radio band and was investigated in detail in the monograph[1]. To observe splitting directly in gases or metal vapors in the optical region of the spectrum, it is necessary that the magnitude of the splitting exceed the Doppler width of the line ($|V| \gg k\bar{v}$, $\bar{v} = (2kT/M)^{1/2}$). The experimental studies[2-5,7] of the Stark effect in the giant fields of a ruby laser leave no doubt as to the existence of level splitting. Nonetheless, the question of the structure of the splitting in such fields and of its connection with the space-frequency characteristics of the laser radiation still seems to remain open at present[17-19].

In gas-laser fields, the Stark level shifts are comparable to or smaller than Γ ($|V| \ll \Gamma$). Owing to the thermal motion, each atom of the ensemble has its own splitting structure, inasmuch as by virtue of the Doppler principle, the field frequencies (2.2) in a coordinate system that is at rest relative to the atom are altered respectively by $\omega_0 - \mathbf{k}\cdot\mathbf{v}$ and $\omega_\mu - \mathbf{k}_\mu\cdot\mathbf{v}$ is the velocity of the atom. The power radiated by the ensemble is obtained from formula (2.8) by averaging over the Maxwellian velocity distribution of the atoms:

$$\frac{d\bar{\mathcal{E}}}{dt} = 2\hbar\omega_\mu |V_\mu|^2 N_g \operatorname{Re}\left\{\int d^3\mathbf{v}\,(\sqrt{\pi}\,\bar{v})^{-3} e^{-\mathbf{v}^2/\bar{v}^2} \times\left[i(\Omega_\mu - \mathbf{k}_\mu\mathbf{v}) + \Gamma_{ng} + \frac{|V|^2}{\Gamma_{gm} + i(\Omega_\mu - \mathbf{k}_\mu\mathbf{v} - \Omega + \mathbf{k}\mathbf{v})}\right]^{-1}\right\}, \tag{2.9}$$

where $\Gamma_{ng} = (\gamma_n + \gamma_g)/2$, $\Gamma_{gm} = (\gamma_m + \gamma_g)/2$, and $\bar{v} = (2kT/M)^{1/2}$.

The integrand in (2.9) is proportional to the energy radiated per unit time by atoms moving with definite velocity. For waves moving in the same direction ($\mathbf{k}\cdot\mathbf{k}_\mu > 0$), the integrand has, generally speaking, two maxima as a function of $\eta = \mathbf{k}_\mu\cdot\mathbf{v}$. At appropriate velocities, the radiation frequency is at resonance with one of the transitions shown by the wavy lines in Fig. 2. This is seen most clearly from the formula obtained from (2.9) by restricting oneself to the first order of perturbation theory in $|V|^2$:

$$\frac{d\bar{\mathcal{E}}}{dt} = 2\hbar\omega_g |V_\mu|^2 N_g (\sqrt{\pi}\,\bar{v})^{-3}\int d^3\mathbf{v} e^{-\mathbf{v}^2/\bar{v}^2}\left\{\left(1 + \frac{k-k_\mu}{k}\frac{k_\mu}{k}\frac{|V|^2}{z^2}\right) \times \frac{\Gamma_{ng}}{(\Omega_\mu - \eta)^2 + \Gamma_{ng}^2} + \left(\frac{k-k_\mu}{k}\right)^2 \frac{|V|^2}{z^2}\,\frac{\Gamma_{gm}}{[\Omega_\mu - \Omega - (k_\mu - k)\,k_\mu^{-1}\eta]^2 + \Gamma_{gm}^2}\right\}; \tag{2.10}$$

here $z = \Omega_\mu - (k_\mu/k)\Omega$, $\Gamma_k = (k_\mu/k)\Gamma_{gm} + [1 - (k_\mu/k)]\Gamma_{ng}$, and it is assumed that $|z| \gg \Gamma_k$.

Let us analyze formula (2.10). There are two groups of particles making the principal contribution to the radiation energy. With increasing $|V|^2$, the number of particles of the first group decreases with $k < k_\mu$, but the number of particles of the second group increases

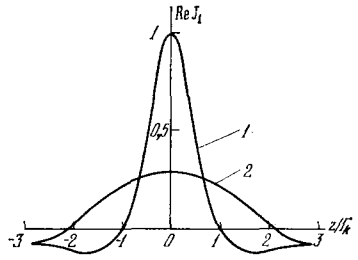

FIG. 3. Plots of the function Re $J_1(\Omega_\mu)$ at the parameters $\kappa_p = 0$ (curve 1) and 1 (2).

by the same factor ($k\bar{v} \gg \Gamma_{ng}, \Gamma_{gm}$). The summary radiation power does not change and the splitting effect does not appear. If $k > k_\mu$, both groups of particles increase with increasing $|V|^2$. By varying ω_μ it is possible to obtain coalescence of the maxima of their velocity distributions. In this case the radiated power should decrease. Accordingly, a fine structure due to the splitting of the n level appears in the form of a dip on the line contour of the g – n transition.

To find the shape of the dip, it is necessary to average in (2.9) over the velocities for parallel k and k_μ. As a result we obtain for the radiated power the formula ($k\bar{v} \gg \Gamma, |V|, \mathbf{k}_\mu\mathbf{k} > 0$)[20]:

$$d\bar{\mathcal{E}}/dt = 2\hbar\omega_\mu |V_\mu|^2 N_g (\pi^{1/2}/k_\mu\bar{v})\, e^{-(\Omega_\mu)^2/(k_\mu\bar{v})^2} \operatorname{Re}[1 - 2\varkappa_p\theta(k - k_\mu) J_1(\Omega_\mu)], \tag{2.11}$$

where

$$J_1(\Omega_\mu) = \Gamma_k^2/2w(\zeta)[(\zeta/2) + w(\zeta)], \quad w(\zeta) = [(\zeta/2)^2 + \varkappa_p\Gamma_k^2]^{1/2}, \quad \zeta = \Gamma_k + iz, \quad \varkappa_p = (k - k_\mu)\,k^{-1}(k_\mu/k)\,|V|^2/\Gamma_k^3. \tag{2.12}$$

In the limiting case $\kappa_p \ll 1$ we have

$$J_1(\Omega_\mu) \approx \Gamma_k^2/[\Gamma_k + i(\Omega_\mu - (k_\mu/k)\Omega)]^2. \tag{2.13}$$

In this approximation, the form of the dip on the Doppler line contour was first obtained in[21,22], and in a more general relaxation model in[23]. The described phenomenon was first observed experimentally in[22].

The parameter κ_p (see (2.12)) can be assumed to be the parameter of "saturation" of the splitting effect. Figure 3 shows plots of the function Re $J_1(\Omega_\mu)$ for $\kappa_p = 0$ and 1. From a comparison of the curves we see that with increasing field the fine structure connected with the splitting of the levels spreads away.

We turn now to a consideration of the singularities of the interaction of the field (2) with atoms initially excited to the level m or n. For a weak field at frequency ω_μ, we can neglect in the second equation of the system (2.3) the term containing the amplitude C_g. The evolution of the amplitudes C_m and C_n in time will now be determined only by the strong field, which leads to oscillations[12] with frequencies (2.6). The absorption of energy at the frequency ω_μ occurs simultaneously with the transition of the atom from the level n to the level g. The maxima of the absorbed energy (see the last equation of the system (2.3)) correspond to the resonances $-\Omega_\mu = \Omega_{1,2}$ and are interpreted as the transitions shown by the wavy lines in Fig. 2.

The power absorbed by an individual atom experiences oscillations with a difference frequency $\Omega_1 - \Omega_2$. The intensity beats are connected with the coherent excitation of the sublevels (2.7) and can be separated by modulating the excitation[24-26].

The only atoms from the ensemble with Maxwellian

velocity distribution that interact with the strong field are those which the detuning $\Omega = \omega_0 - \omega_m$ is compensated by the frequency shift due to the Doppler effect ($\Omega = kv$). As is well known[8], stimulated transitions cause a redistribution of the particles over the levels m and n. A Bennett beam is produced with a velocity distribution (1.1).

The averaging of expression (2.4) for the energy absorbed per unit time over the Maxwellian distribution at $k\bar{v} \gg \max(\Gamma_B, \Gamma_{ng}, \Gamma_{gm})$, reduces to averaging over the Bennett distribution, i.e., to averaging over the group of atoms that interact most actively with the field. If it is assumed that the pump Q_l at the level l = m, n, g does not depend on the time, it is quite easy to obtain from (2.3) and (2.4) the following expression for the energy absorbed (radiated) per unit time[27,28] ($k < k_\mu$):

$$\frac{d\bar{\mathcal{E}}^{\pm}}{dt} = 2\hbar\omega_\mu |V_\mu|^2 \frac{\pi^{1/2}}{k_\mu \bar{v}} e^{-\Omega_\mu^2/(k_\mu\bar{v})^2} \operatorname{Re}\left\{N_g - N_n - (N_m - N_n)\frac{k_\mu}{k}\frac{2|V|^2}{(1+\varkappa)^{1/2}}\frac{[(\Gamma_\pm + iz)/\gamma_n] + \{[1 \pm (1+\varkappa)^{1/2}]/2\}}{(\Gamma_0 + iz)(\Gamma_\pm + iz) + |V|^2}\right\}; \quad (2.14)$$

the plus and minus signs in (2.14) correspond to k_μ directed parallel and antiparallel to k, $N_l = Q_l/\gamma_l$ (l = m, n, g),

$$\Gamma_0 = \Gamma_{ng} + (k_\mu/k)\Gamma_B, \quad \Gamma_\pm = \Gamma_{gm} + [(k_\mu/k) \mp 1]\Gamma_B, \quad z = \Omega_\mu \mp (k_\mu/k)\Omega. \quad (2.15)$$

Formula (2.14) has the same structure as the analogous expression for the immobile atom[1], the resonant frequency of which has been calculated in terms of the maximum of a Bennett distribution with widths $\Gamma_\pm$ and Γ_0 instead of Γ_{gm} and Γ_{ng} (the model of "effective" immobile atoms[28]). The change of the widths is easily understood. For an immobile atom in the limit as $V \to 0$, the widths of the transitions shown by the wavy lines in Fig. 2 are Γ_{gm} and Γ_{ng}. When averaging over the distribution (1.1), the quantities Γ_0 and $\Gamma_\pm$ should be made up of Γ_{ng} and Γ_{gm} and the width of the distribution (1.1) with respect to the velocities $\delta v = \Gamma_B/k$, recalculated in terms of the corresponding frequency shifts:

$$\Gamma_0 = \Gamma_{ng} + k_\mu \delta v = \Gamma_{ng} + (k_\mu/k)\Gamma_B$$

and (see, e.g., (2.9))

$$\Gamma_\pm = \Gamma_{gm} + (k_\mu \mp k)\delta v = \Gamma_{gm} + [(k_\mu/k) \mp 1]\Gamma_B.$$

Thus, the anisotropy of the widths of the "effective" immobile atom is simply a manifestation of the Doppler effect.

It is seen from (2.14) that a fine structure appears on the Doppler line contour of the g – n transition even in the first nonvanishing order of perturbation theory in the strong field[29]. In the case of observation along k (Fig. 4), this is a spike (dip) having a Lorentz shape and a width $\Gamma_\pm$, as well as a maximum (minimum) at the frequency $\Omega_\mu = (k_\mu/k)\Omega$. In the case of observation in the opposite direction, a spike (dip) of Lorentz shape is likewise observed, but its width is now Γ_0 and the maximum (minimum) is at the frequency $\Omega_\mu = -(k_\mu/k)\Omega$. The centers of the spikes (dips) are shifted relative to the line center by the Doppler effect. This constitutes emission or absorption of atoms moving along k with a velocity distribution (1.1) (Bennett beam)[1)].

The width of the Bennett distribution (1.1) and, consequently, also the widths of the "effective" atom, increase with increasing strong-field intensity. In the spontaneous-relaxation approximation and at $\gamma_{mn} \ll \gamma_m v(\gamma_{mn}$ is the Einstein coefficient of the m – n transition), no Stark splitting of the fine structure takes place[27]. There is only an increase of the widths of the spikes (dips) in proportion to $(\gamma_g/2) + [(k_\mu/k)\Gamma \mp (\gamma_n/2)](1+\varkappa)^{1/2}$, starting with the minimal values $(\varkappa = 0)\ \Gamma_+ = \Gamma_{gm} + [(k_\mu/k) - 1]$ and $\Gamma_0 = \Gamma_{ng} + (k_\mu/k)\Gamma$.

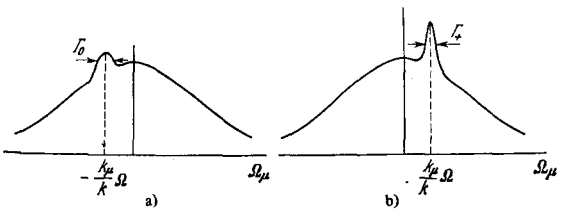

FIG. 4. Spikes produced on the Doppler contour of the emission line of the g-n transition in the direction oposite to the propagation direction of the strong field (a) and in the propagation direction of the strong field(b). Figures a and b should be interchanged for m - n - j cascade transitions.

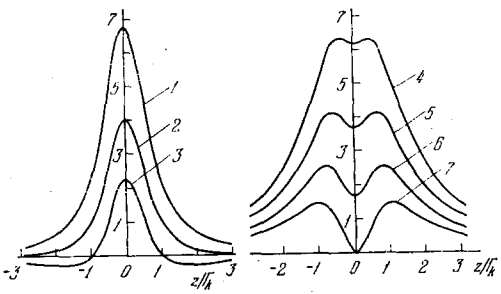

FIG. 5. Plots of the functions $\tilde{I}(z) = \langle[(\xi/\epsilon) - 1]^2 + 4\rangle^{1/2} I(z)$ for values of the parameter ξ/ϵ = 2 (curve 1), 1 (2) and 0 (3), and of the function $\tilde{I}(z) = -\langle[(\xi/\epsilon) - 1]^2 + 4\rangle^{1/2} I(z)$ for values of the parameter ξ/ϵ = –2.5 (4), –2 (5), –1.5 (6) and –1 (7).

At $k_\mu \approx k$ and $\gamma_g, \gamma_m \ll \gamma_n$ the widths of the spikes or dips produced on the Doppler line contour differ greatly when observed along and against the propagation direction of the strong field. The minimum width Γ_+ of the singularity turns out to be smaller than the natural width Γ_{ng} of the g – n transition. The cancellation of the Doppler shifts in this case[31] is completely analogous to their cancellation in the case of forward Rayleigh scattering[32].

The considered fine structure of the Doppler-broadened line was first predicted theoretically for spontaneous emission in[29] and observed experimentally by Holt[30].

Formula (2.15) was derived under the assumption that $k_\mu > k$. If the ratio of the wave-vector lengths is reversed ($k_\mu < k$) for waves having the same direction ($k_\mu \cdot k > 0$), then the fine structure (2.11), due to the same level splitting (2.7), is superimposed on the Lorentz-shape spike (dip) in the vicinity of the frequency $\Omega_\mu = (k_\mu/k)\Omega$. In this case we have in the first nonvanishing order of perturbation theory in the strong field (see, incidentally,[20])

$$\frac{d\bar{\mathcal{E}}}{dt} = 2\hbar\omega_\mu |V_\mu|^2 \frac{\pi^{1/2}}{k_\mu \bar{v}} e^{-\Omega_\mu^2/(k_\mu\bar{v})^2}\left[N_g - N_n - (N_m - N_n)\frac{2|V|^2}{\gamma_n\Gamma_k}\varepsilon\frac{k_\mu}{k} I(z)\right],$$

where

$$I(z) = (\varepsilon^{-1} - 1)[\Gamma_k^2/(\Gamma_k^2 + z^2)] + 2[\Gamma_k^2/(\Gamma_k^2 + z^2)]^2,$$
$$\varepsilon = [(N_g - N_n)/(N_m - N_n)](k - k_\mu)\gamma_n/k\Gamma_k,$$
$$\Gamma_k = (k_\mu/k)\Gamma_{gm} + [1 - (k_\mu/k)]\Gamma_{ng}.$$

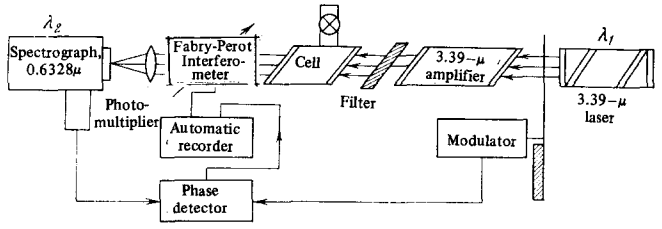

FIG. 6. Experimental setup for the investigation of the line shape of spontaneous emission on the $3s_2-2p_4$ transition of neon in the presence of a field on the adjacent transition $3s_2-3p_4$ [41].

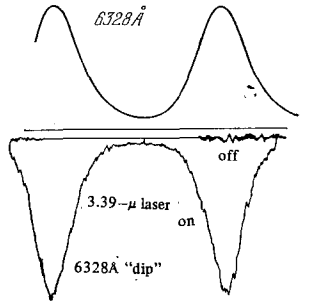

FIG. 7. Line shape of 0.63-μ spontaneous emission.

The shape of the singularity in the Doppler line contour of the g – n transition is now determined by the function I(z). Plots of this function are shown in Fig. 5. Their analysis shows that the shape of the singularity depends significantly on the ratio of the population difference $N_g - N_n$ to $N_m - N_n$. The change of the line shape is due to one cause only in the limiting cases $1/\epsilon = \pm\infty$ or $1/\epsilon = 0$.

In the exposition of the theory of the fine structure of a Doppler-broadened spectral line it was assumed that the relaxation of the atomic system is determined only by spontaneous processes and that the cascade population of the level n from the level m can be neglected ($\gamma_{mn} \ll \gamma_m$). Generalization of the theory to include the case when collisions and cascade processes play a role has been the subject of[28,33-35]. It is shown there that the fine structure due to the external field is quite sensitive to these processes, and its investigation allows us to assess the character of collisions. The effect of the recoil of the radiating atom on the shape of the fine structure was considered in[35]. The singularities of nonlinear phenomena in the standing wave were analyzed in[36]. Several papers[37,38] are devoted to the interpretation of the considered nonlinear phenomena.

3. EXPERIMENTAL INVESTIGATIONS OF THE FINE STRUCTURE

Interest in the use of Bennett beams for the purposes of high-resolution spectroscopy arose relatively long ago[39,40]. But the first experiments in which the existence of Bennett dips in the atom velocity distributions and consequently the onset of the fine structure in the emission line was directly demonstrated were not published until five years had passed following Bennett's paper[8].

Bennett, Chebotayev, and Knutson[41] investigated the line shape of spontaneous emission on the transition $3s_2 - 2p_4$ (m – l) of neon ($\lambda = 0.63$ μ) in the presence of a field at the adjacent transition $3s_2 - 3p_4$ (m – n) ($\lambda = 3.39$ μ). The experimental setup is shown in Fig. 6. A short single-mode He-Ne laser, emitting at 3.39 μ, was tuned to the center of the amplification line. The output radiation, which constituted a traveling wave, was modulated at a frequency 30 Hz and amplified in an He-Ne discharge to an approximate level 100 μW. The modulated radiation was then passed through a 3.39-μ filter, which cut off the 0.63 μ radiation, and entered an interaction cell excited by a high-frequency discharge in an He-Ne mixture. The visible light of wavelength 0.63 μ, emitted spontaneously, was analyzed with a scanned Fabry-Perot interferometer. The electric signal from the photomultiplier was fed to a phase-sensitive receiver, which used the modulation frequency as a reference frequency. The signal from the output of the phase-sensitive receiver, containing information on the 0.63-μ spontaneous emission in the 3.39-μ radiation field, was registered with an automatic x-y recorder and plotted as a function of the frequency.

Typical experimental results are shown in Fig. 7. The upper trace is the 0.63-μ emission spectrum in the case when the 3.39-μ laser is covered, and is none other than the Doppler-broadened spontaneous-emission line of the He-Ne discharge on the 0.63 μ line of Ne. The lower trace is the spontaneous-emission line dip due to the action of the 3.39-μ radiation field. Plots of two orders were obtained for the purpose of illustrating the reproducibility of the results and the frequency calibration of the horizontal sweep of the automatic recorder.

The obtained curves were used by the authors to determine the Lorentz shape for $3s_2 - 3p_4$ and $3s_2 - 2p_4$ transitions of Ne and their broadening as functions of the He and Ne pressures. In the indicated experiments, owing to the large homogeneous width of the 3.39-μ line, the spectral width of the structure produced in the external field turned out to be quite large. Nonetheless, it was proven beyond a doubt in this paper that Bennett dips exist in the velocity distributions of the atoms[8].

In[42,43] they investigated spontaneous emission from a resonator, observed along the laser-radiation propagation axis. Cordover et al.[42] were the first to demonstrate the application of the saturation effect for extremely accurate measurements of isotopic shifts of two optical transitions in neon. They obtained a complete resolution of the isotropic structure, which is masked under ordinary conditions by Doppler broadening. In this experiment they used a short single-mode He-Ne laser emitting at $\lambda = 1.15$ μ ($2p_4 - 2s_2$ transition of Ne). The spontaneous emission at 0.6096 μ ($2p_4 - 1s_4$), which starts from the lowest laser level, was observed through one of the mirrors, which transmitted in the 0.6-μ region. The spontaneous-emission spectrum was analyzed with the aid of a pneumatically adjustable Fabry-Perot interferometer and was registered by a photomultiplier with a diaphragm for mode selection.

Figure 8 shows the spectrum of the spontaneous emission from the level $2p_4$, observed along the laser axis. The upper trace in Fig. 8a corresponds to the usual Doppler-broadened line contour of spontaneous emission at 0.6096 μ for the Ne^{20} isotope. The middle and lower traces show the fine structure produced in the presence of a field at 1.15 μ when the generation frequency is tuned to the center of the amplification line and detuned from it, respectively. The splitting of the fine structure of the spontaneous-emission line into two components can be easily understood by recognizing that the electromagnetic field in the Fabry-Perot

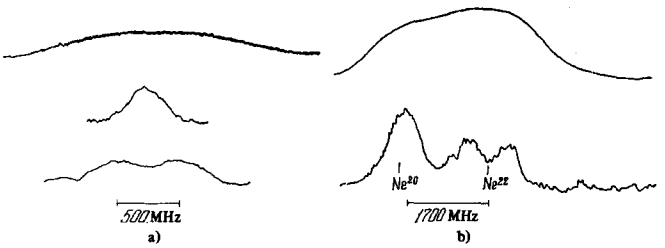

FIG. 8. 0.6096–μ spontaneous-emission line shape ($2p_4 - 1s_4$ transition of Ne) from the resonator of a 1.15–μ He-Ne laser for the isotope Ne^{20} (a) and for a mixture of the isotopes Ne^{20} and Ne^{22} (b).

resonator is a standing wave. The latter can be represented as a superposition of two traveling waves of equal velocity. Each wave produces its own Bennett beam. If the radiation is observed along the resonator axis ($|\Omega| \gg \Gamma$), one beam travels towards the observer and the other moves away in the opposite direction (see Formula (1.1)). When $\Omega = 0$, the maxima of the Bennett beams coincide and the spikes on the Doppler contour coalesce.

The observed fine structure in the spontaneous-emission line (Fig. 8a) was used to determine the isotopic shift of the 1.15-μ and 0.6096-μ lines of Ne. The measurements were performed using an He-Ne laser filled with a mixture of the atoms Ne^{22} and Ne^{20} in a 3 : 2 ratio. Owing to the Doppler broadening, the isotopic components for the 1.15 and 0.6096 μ lines are usually not resolved (see the upper curve of Fig. 8b). The spontaneous emission in the external field was observed under conditions when the generation frequency coincided with the frequency of the $2s_2 - 2p_4$ transition for the Ne^{20} isotope. The fine structure for the Ne^{20} isotope therefore had the form of a single narrow peak. At the same time, the isotopic shift for the 1.15-μ line caused the generation frequency to be tuned away from the central frequency of the transition for the Ne^{22} isotope, by an amount equal to the isotopic shift. The detuning split the fine structure (lower trace in Fig. 8b). As a result, the trace in Fig. 8 contains information on the isotopic shifts of the two transitions $2s_2 - 2p_4$ and $2p_4 - 1s_4$ of Ne. The measured isotopic shift of 0.6 μ turned out to be 1706 ± 30 MHz, and that for the 1.15 μ line was 257 ± 8 MHz, the frequency for Ne^{20} being shifted into the red region of the spectrum.

An experiment almost completely identical with[42] but without measuring the isotopic shifts was performed independently in[43]. The same system of transitions was used there, with only slight differences in the experimental setups.

In the considered experiments, the fine structure of the line produced in the presence of the generation field of a gas laser was interpreted by using only the effect of formation of a nonequilibrium velocity distribution in a monochromatic field (Bennett beams). The first rigorous analysis of the line shape of spontaneous emission of a gas in the presence of a monochromatic optical field at the adjacent transition was carried out in[29]. It was indicated there, for the first time, that the fine structure of the spontaneous-emission line exhibits anisotropy for observation along and against the direction of the strong-field propagation (see Fig. 4).

The first qualitative experimental confirmation of the theory of[29] was obtained by Holt[30]. She investigated the fine structure of the spontaneous emission in

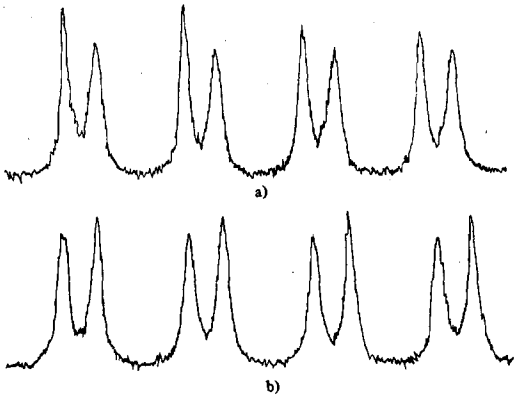

FIG. 9. Experimental confirmation of the asymmetry of the line of spontaneous emission from a gas-laser resonator [30].

the same system of transitions as in[42,43]. By improving the procedure for registering the fine structure, it was possible to increase the signal/noise ratio and to observe the asymmetry of the emission line in the presence of the standing-wave field.

The experimental accuracy was limited by shot noise, by the drift of the laser frequency, and by the resolution of the Fabry-Perot interferometer. The small amplitude of the signal was due to the fact that the laser was operated near the threshold to ensure a single-frequency generation regime. In addition, it was necessary to use spontaneous emission in a very small solid angle along the laser axis. Thus, a deviation of 0.025 rad from the axis led to a peak broadening of 17 ± 4 MHz. Since the laser had to be detuned from the center of the amplification line to obtain separation of the peaks, it was not stabilized. The laser frequency drift imposed a lower limit on the scanning rate of the Farby-Perot interferometer. The scanning rate was 6 min/order. For the data used in the analysis, the laser frequency changed by not more than 5 MHz in one order. The apparatus width due to the system comprising the Fabry-Perot interferometer and the monochromator was 95 ± 10 MHz and was measured with the aid of a laser with emission wavelength 0.63 μ. The base of the interferometer was 6.6 cm long in order to obtain a sufficiently large spectral interval (2275 MHz).

Figure 9 shows typical plots of the spontaneous-emission spectrum obtained by Holt. Several orders of the interferometer are shown to demonstrate that the difference in the peak amplitudes is not due to the laser-frequency drift. Figure 9a corresponds to a detuning $\Omega = 160$ MHz, and Fig. 9b to $\Omega = -170$ MHz as reckoned from the center of the Lamb dip. Within the limits of the measurement errors, each peak is described by a Lorentz contour. This means that the fine structure due to the external field also has a Lorentz shape, since the apparatus function of the interferometer is a dispersion curve. The fine-structure width of interest to us can be obtained simply by subtracting the appratus width of the interferometer from the measured width of the peak.

Unlike the experiments of[42,43], the fine structure observed in[30] on the spontaneous-emission contour and produced in a standing-wave field is asymmetrical, the sign of the asymmetry depending on the sign of the detuning Ω of the frequency relative to the center of the amplification line. A change of the sign of the detuning Ω leads to a change in the character of the asym-

metry. It is easy to verify that the onset of symmetry is due precisely to the dependence of the spontaneous-emission line shape on the observation direction (Fig. 4). Experiments show that in the case of the cascade transition scheme m → n → j the line fine structure due to the wave propagating away from the observer is sharper than that due to the wave propagating in the direction of the observer. This character of the spontaneous emission in the presence of an external monochromatic field on the adjacent transition coincides fully with the predictions of the theory[29]. The measured difference of the peak amplitudes turned out to be equal to 14 ± 2%, and the difference of the measured widths was 15 ± 4%. Holt's experiments confirmed qualitatively the predictions of the theory. To be sure, an analysis of the peak widths and an attempt to determine the transition and level relaxation constants even led to a negative value of the width of one of the levels. This was more readily due to the influence of collisions, which were not taken into account in the theories[29,30].

The first experiments to investigate stimulated-emission line shape in the presence of a strong field on an adjacent transition[22,44] have also demonstrated a definite discrepancy between the existing theory and experiment, although they confirmed beyond any doubt the presence of anisotropy of the emission line. In these experiments they used the transitions $2s_2 - 2p_4$ ($\lambda = 1.15\ \mu$) and $3s_2 - 2p_4$ ($\lambda = 0.63\ \mu$) of Ne with a common level $2p_4$, but under different conditions. The experiment of[44] was devoted to an investigation of the generation-line shape of a three-level gas laser, i.e., a laser in which the amplification is attained by pumping with monochromatic radiation. Since a monochromatic field interacts in a gas only with atoms whose velocity projections on the field propagation direction lie in a narrow interval $\Delta v \sim \Gamma/k$, the amplification and generation in such a laser were effected, as it were, by the atomic beam. This makes it possible to obtain exceedingly narrow amplification lines.

A gas laser in which the amplification necessary for generation is produced by an external monochromatic field (Fig. 10) should have a number of features that distinguish it from ordinary gas lasers with incoherent pumping. These features will affect primarily the generation line shape[28,45]. The unsaturated gains for each of the traveling waves making up the standing wave in the Fabry-Perot interferometer are, generally speaking, different. This difference is a consequence of the anisotropy of the amplification line (see formula (2.14)) in the presence of an external field. In the case when the excess over threshold is due only to the pumping by an external field, two generation regions occur ($|\Omega|/\Gamma > 1$), corresponding to spikes on the Doppler line contour (see Fig. 4). With decreasing $|\Omega|$, these regions come close together. The gain is correspondingly increased. The sharp dependence of the gain on the detuning is analogous to that predicted for a beam laser[46].

Investigations of the generation line shape of a three-level gas laser at 1.15 μ in the presence of a pumping

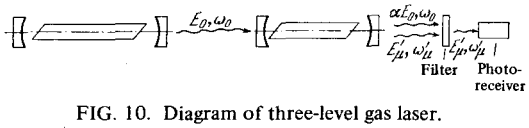

FIG. 10. Diagram of three-level gas laser.

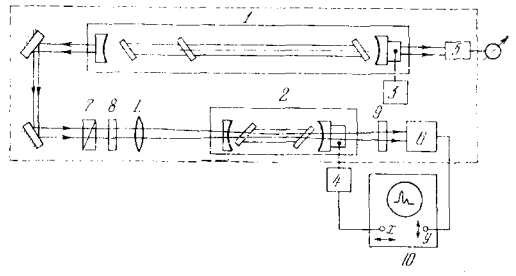

FIG. 11. Experimental setup for the investigation of the generation line shape in a three-level gas laser. 1—He-Ne laser ($\lambda = 0.63\ \mu$), 2—tunable Fabry-Perot resonator for $\lambda = 1.15\ \mu$, 3,4—blocks for controlling the piezoceramic, 5, 6—photodiodes, 7, 8—optical "decoupling", 9—optical filter, 10—recording device.

field on the transition $3s_2 - 2p_4$ ($\lambda = 0.63\ \mu$)[44,45] were carried out with the experimental setup shown in Fig. 11. The radiation from a high-power (8 MW) single-frequency He-Ne laser ($\lambda = 0.63\ \mu$), with mode selection by an internal absorbing cell[47], was passed through an external absorbing cell. This cell was placed inside a resonator made up of interference mirrors (reflection coefficient 98.5) tuned to the wavelength $\lambda = 1.15\ \mu$ with maximum possible transmission (~80%) at the wavelength of the external field, making it possible to disregard the reflection from the mirror and to regard the pumping field with sufficient accuracy as a traveling wave. The distance between the mirrors was 20 cm, i.e., $c/2L = 750$ MHz. The external absorbing cell was a discharge tube with discharge-section length 11 cm and diameter 2 mm, and was filled with Ne^{20}. The polarizations of the pump field and of the generation field were linear and coincided in angle. The coupling between the resonators was eliminated either with a polarization filter or by slight detuning of the optical axes of the resonators. The fields were matched by starting from the requirement of maximum coincidence of the wave fronts and the beams, although complete matching was impossible, owing to the difference in the wave numbers. The 1.15-μ radiation was registered with germanium photodiodes. The external-field radiation passing through the resonator of the three-level laser was filtered out with an IKS-1 infrared filter. The signal from the photodetector was fed to an oscilloscope or an automatic recorder. The horizontal sweep was by the same sawtooth or sinusoidal voltage as applied to the piezoceramic element used to vary the length of the three-level laser resonator. The generation power was seen to have a frequency dependence due to the external field.

Figure 12 shows the experimentally observed generation line shape at fixed frequency detunings of the external field relative to the center of the absorption line. Measurements of the width of the generation region with a gain equal to double the threshold have shown that the amplification line width at a pressure $p_{Ne} = 0.3$ mm Hg is equal to $2\Gamma_0 = 75 \pm 5$ MHz, which is smaller by one order of magnitude than the Doppler width $k_\mu \bar{v} = 800$ MHz at 400°K. At the same time, in spite of the noticeable amplitude asymmetry at $|\Omega| > \Gamma$, the widths of the generation regions measured in analogous fashion turned out to be equal within the limits of the measurement errors. Calculation using the known radiation constants yielded widths $2\Gamma_0 = 49.4$ MHz and $2\Gamma_+ = 40.2$ MHz, with a difference of about 20%. The value extrapolated to zero pressure was $2\Gamma_0 \approx 2\Gamma_+ \approx 59 \pm 5$ MHz. Extrapolation to zero field was not carried out, owing

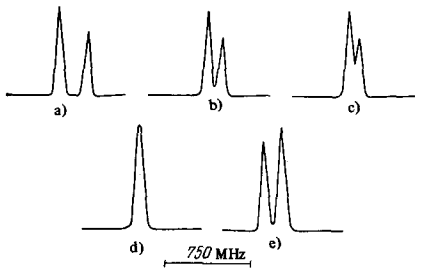

FIG. 12. Generation line shape of three-level gas laser. Ω(MHz) ≈ -194 (a)–100 (b),–67 (c), 0 (d), and 119 (e).

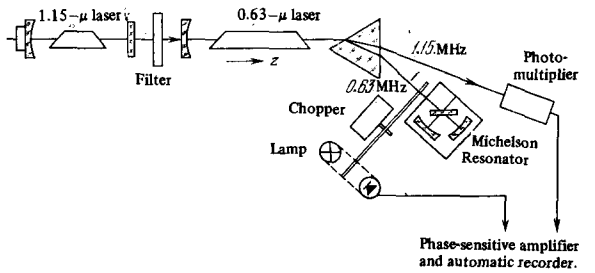

FIG. 13. Experimental setup for the observation of the gain saturation effect.

to the large measurement errors in weak fields.

The generation-line shape coincides with the line shape of the unsaturated gain only when the parameter of saturation in the field does not depend on the frequency. Since there was no rigorous theory of a three-level laser at that time, only qualitative inferences concerning the saturated-gain line shape could be drawn on the basis of the generation line shape.

Using the same transitions but a different experimental setup and less pure conditions (discharge in a mixture of He and Ne gases), Hansch and Toschek (see[22]) observed not only the asymmetry of the stimulated-emission line shape in the field of a standing wave at $|\Omega| > \Gamma$, but also a difference between the line widths corresponding to different directions of propagation of nonlinearly interacting waves of the weak and strong field.

An experimental investigation of the interaction of coupled laser transitions was carried out for the purpose of studying elastic collisions processes[48] and consisted of the following. The output radiation of a short single-frequency He-Ne laser with wavelength 1.15 μ was passed through a long (1.5 m) single-frequency He-Ne laser with wavelength 0.63 μ, in which mode selection was effected with an interferometer of the Michelson type[49] (Fig. 13). To ensure separation of the beams with different wave numbers, a quartz prism was inserted in the resonator of the 0.63-μ laser. The 0.63-μ field was modulated with a mechanical chopper. Consequently, unlike the experiments described above[44], there was amplification on both transitions, and the presence of a strong field at 0.63 μ led to a decrease of the gain of the weak field for 1.15 μ. In this case the strong field was in the form of a standing wave and the weak field in the form of a traveling wave.

The interpretation of the observed phenomena coincides exactly with the case of spontaneous emission from a gas-laser resonator[30,42,43], but what is now investigated is not spontaneous emission but the line shape of stimulated emission with the aid of a weak sounding signal.

Figure 14 shows the experimentally observed amplification-line shape of a weak field at 1.15 μ in the presence of a strong 0.63 μ radiation field. The left-hand beam corresponds to the interaction of waves traveling in the same direction, and the right-hand beam to oppositely directed waves. Since the $2s_2$ and $3s_2$ levels are optically coupled with the ground state $1s_0$ of neon, the asymmetry should be relatively small (~20%) and should decrease further with increasing total pressure. The experiment revealed a relatively

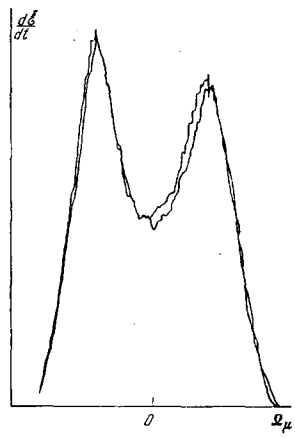

FIG. 14. Line shape of stimulated emission at 1.15μ in the presence of a standing wave with 0.63μ.

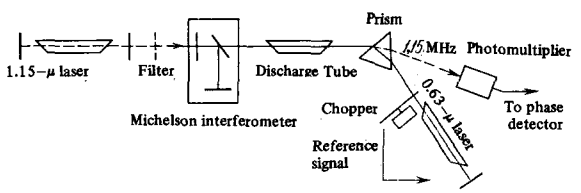

FIG. 15. Experimental setup for the observation of the splitting effect.

large asymmetry, which did not agree with the results of[44] or with the concept developed by that time in the theoretical papers. Nonetheless, the total narrowing of the emission line was small and did not agree quantitatively with calculations from the known relaxation constants of the transitions.

Many unclear problems have been explained since the effect interpreted by the authors as a manifestation of the dynamic Stark effect[22] was observed experimentally. This phenomenon is of importance when the frequency of the strong field exceeds the frequency of the weak field ($k > k_\mu$) and the propagation directions of the two coincide (see formulas (2.11) and (2.13)). In this case a change in the emission line shape takes place even in those cases when the strong field is not absorbed ($N_m = N_n$).

To observe this effect, the experimental setup was modified in[22]. An additional discharge cell (Fig. 15) was introduced into the resonator of a 0.63-μ laser. By adjusting the partial and total pressures of the He and Ne, and also the discharge current, it was possible to obtain a regime in which the strong-field absorption coefficient was equal to zero. It is through this cell that the weak sounding signal with wavelength 1.15 μ was transmitted.

Figure 16 shows three spectra of the weak 1.15-μ

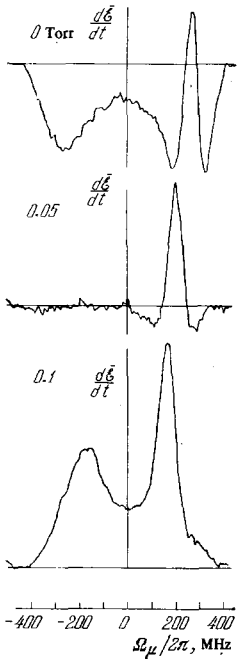

FIG. 16. Splitting effect[22]. The number on the left of each curve indicates the helium pressure.

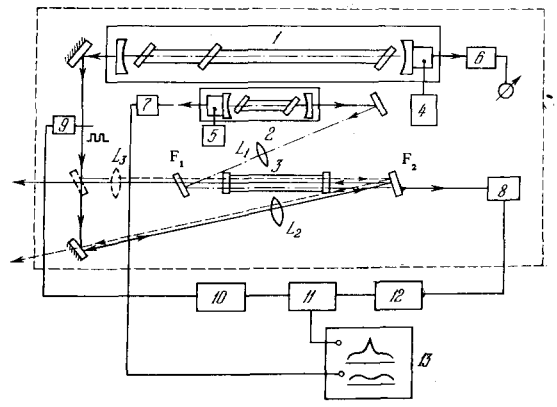

FIG. 17. Experimental setup for observation of the anistropy of the fine structure of a stimulated emission line. 1–He-Ne laser with $\lambda = 1.52\mu$ (strong field); 2–He-Ne laser with $\lambda = 1.15\ \mu$(weak field); 3–discharge cell; 4, 5–blocks for control of the piezoceramic; 6-8–photodiodes, 9–mechanical chopper; 10–acoustic generator; 11–phase-sensitive detector; 12–selective amplifiers; 13–automatic recorder.

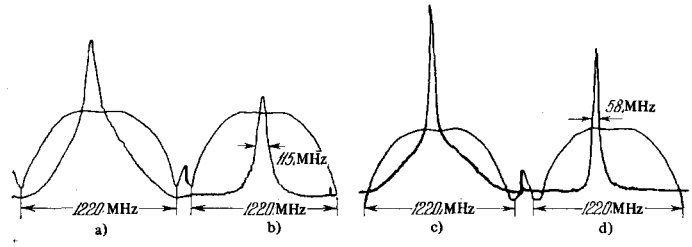

FIG. 18. Line shape of stimulated emission with $\lambda = 1.15\ \mu$ ($2s_2 - 2p_4$) in Ne in the presence of a strong field at the adjacent transition $2s_2 - 2p_1$ with $\lambda = 1.52\ \mu$.

sounding signal due to the 0.63 standing-wave field when the strong field is detuned from the central transition frequency. The structures on the right and on the left correspond to the nonlinear interaction in the directions parallel and antiparallel to the traveling waves, respectively. There is amplification on the 1.15-μ line in the entire range of He pressures, whereas the population difference on the $3s_2 - 2p_4$ transition reverses sign; the upper trace corresponds to absorption and the lower trace to amplification.

The fine structure observed in the case when the population difference is equal to zero shows that the change of the spectral transition probability as a result of the Stark splitting of the levels (see (2.11)) does not vanish in the case of a Maxwellian velocity distribution; this agrees with the predictions of the theory.

* * *

An important stage in the organization of the experiments was the changeover from investigations of the line shapes of the spontaneous and stimulated emission of the active medium of gas lasers to direct investigations of the line shapes of the spontaneous[50] and stimulated[51-53] emission in external absorbing cells. This has made it possible to extend the range of investigated pressures greatly and to study the dependence of the line shape on the observation direction directly. In[50-54], attention was concentrated not on confirmation of the existence of anisotropy of the emission line, but now on the spectroscopic aspect, i.e., on the possibilities that these effects offer for the solution of fundamental spectroscopic problems.

The 1.15-μ stimulated-emission line shape (transition $2s_2 - 2p_4$ of Ne) was investigated in detail in[51-53] in the presence of a strong monochromatic traveling-wave field at 1.52 μ (transition $2s_2 - 2p_1$ of Ne). At these transitions one could expect the appearance of a fine structure having a characteristic width that is comparable with or even smaller than the natural width of the $2s_2 - 2p_4$ transition. The experimental setup used in[51-53] is shown in Fig. 17. An external monochromatic field with $\lambda = 1.52\ \mu$ was produced by a powerful He-Ne laser in which mode selection was effected by an absorbing cell with discharge in neon. The laser beam was directed to a discharge tube filled with the pure isotope Ne^{20}. To measure the absorption or amplification line shape on the $2s_2 - 2p_4$ transition, a weak field with $\lambda = 1.15\ \mu$ from a short scanned single-mode He-Ne laser was introduced into the same cell either in the same direction as the strong field (the ray path in this case is designated by the dashed line) or in the opposite direction. The optical system ensured matching of the wave fronts of the two beams in the absorbing cell. A mechanical chopper modulated the strong (1.52-μ) field and was synchronized with a phase-sensitive detector. An optical interference filter permitted only radiation with $\lambda = 1.15\ \mu$ to reach the photodiode. The weak-field radiation frequency was scanned slowly. The ac component of the output signal of the photodiode was fed through a selective amplifier and a synchronous detector to one of the channels of the automatic recorder. The second channel of the recorder registered the change of the weak-field amplitude during the course of the frequency scanning. The ac signal at the output of the synchronous detector was proportional to the weak field. It is therefore clear that the ratio of the first spectrogram of the automatic recorder to the second was proportional to the ac part of the absorption coefficient at the Ne line with $\lambda = 1.15\ \mu$, and this part was due to the strong external field with $\lambda = 1.52\ \mu$. The attained signal/noise ratio was 20 dB.

The observed emission line shape is shown in Fig. 18 for the case of oppositely traveling waves (Figs. 18a, b) and for the case when the waves of the weak and strong field propagate in the same direction (Fig. 18c, d). The amplification-line shape has a rather compli-

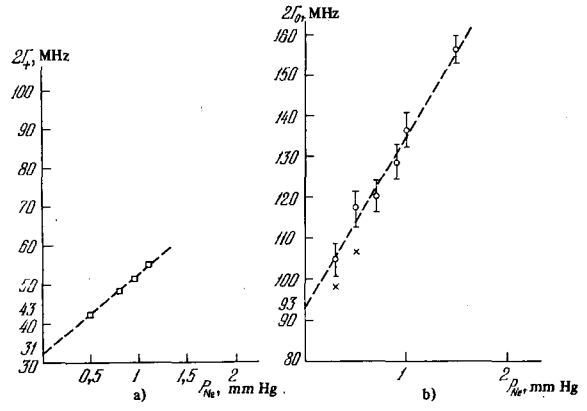

FIG. 19. Dependence of the width of the fine structure on the pressure at $\mathbf{k}_\mu \cdot \mathbf{k} < 0$ (a) and $\mathbf{k}_\mu \cdot \mathbf{k} > 0$ (b).

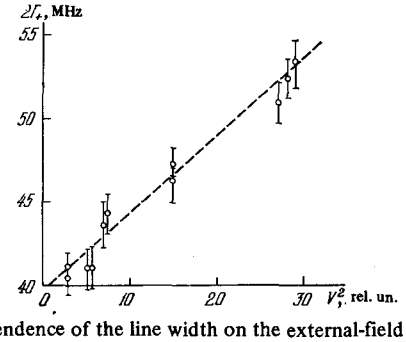

FIG. 20. Dependence of the line width on the external-field intensity

cated form and constitutes a narrow peak against the background of a rather broad "pedestal." For parallel-traveling waves ($\mathbf{k}_\mu \cdot \mathbf{k} > 0$), the peak is much narrower (by about 2 times) (Fig. 18c, d) than for the oppositely traveling waves ($\mathbf{k} \cdot \mathbf{k}_\mu < 0$) (Fig. 18a, b). The broad part is due to the diffusion of the excited $2s_2$ atoms in velocity space, has a Gaussian shape with a width equal to the Doppler width of the line, and is due to the dragging of the resonant radiation on the $2s_2 - 1s_0$ (630 Å) transition and to collisions of the resonant-exchange type in dipole-dipole interaction[52,53]. Figure 18b, c show plots obtained after the broad "pedestal" was eliminated by modulating the discharge in the absorbing cell in counterphase to the strong-field modulation.

The peak widths calculated for this system of transitions by using the radiative constants of the 2s and 2p levels measured in different experiments turned out to be $2\Gamma_+ = 30.8$ MHz (Fig. 19a) and $2\Gamma_0 = 82.6$ MHz (Fig. 19b). The experiment was compared with the theoretical calculations for the first time. For this purpose, the pressure-induced broadening and the field broadening were investigated in (Figs. 19 and 20).

The widths extrapolated to zero field and to zero pressure turned out to be $2\Gamma_0 = 86 \pm 3$ MHz and $2\Gamma_+ = 31.5 \pm 2$ MHz. The values obtained were in good agreement with the calculated ones, and this enabled the authors of[52] to conclude that the theory had been quantitatively confirmed.

In the same experiments, we investigated the polarization of the radiation, and found that the observed sharp structure depends on the level degeneracy and on the state of polarization of the fields. By way of illustration, Fig. 21 shows the measured degree of polarization as a function of the azimuthal angle between the planes of polarization of the weak and strong fields.

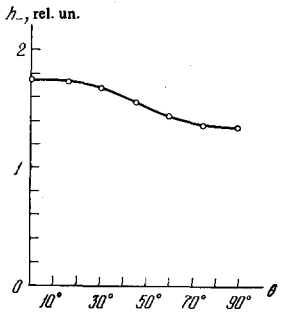

FIG. 21. Polarization anisotropy of the fine structure of the stimulated-emission line.

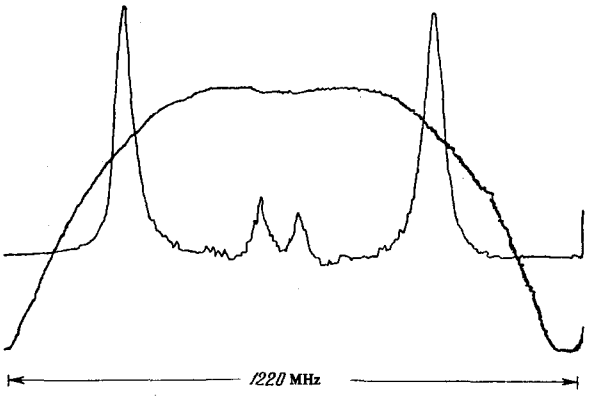

FIG. 22. Zeeman effect in a three-level system.

The observed maximal degree of polarization of the scattering line is 25%. The polarization anisotropy is described with sufficient accuracy by the relation

$$G_\theta/G_0 = 1 - (1/4)\sin^2\theta,$$

where G_0 is the gain for coinciding linear polarizations. If a circularly polarized external field is used, the ratio of the amplitudes for the right- and left-polarized waves of the weak field turned out to be 1 : 6, which agrees (within the limits of measurement accuracy) with the ratio of the probabilities of the dipole transitions between the magnetic sublevels on the transition $J = 1 \rightarrow J = 2$.

The extent to which the use of the fine structure produced in the presence of an external monochromatic field at the adjacent transition is effective in resolving the line structure that is masked under ordinary conditions by the considerable Doppler broadening was demonstrated in[38] with the Zeeman effect as an example. Figure 22 shows a plot of such a structure. When the magnetic field is applied, the line is split even in relatively weak fields. The observed structure was used in[38] to determine the g-factors of the levels $2s_2$ and $2p_4$.

The hyperfine structures of the 1.15- and 0.63-μ lines of the odd isotope Ne^{21} were investigated in[54], and the electric quadrupole moment of the nucleus was measured.

CONCLUSION

The considered nonlinear phenomena that arise when monochromatic radiation interacts with atomic systems can serve as a basis for new methods of high-resolution spectroscopy. At the present time, experimental capabilities are limited to the set of frequencies available from lasers. There are grounds for hoping that the de-

velopment of highly monochromatic radiation sources with tunable frequency will eliminate this limitation completely. The use of lasers makes realistic the extraction of spectroscopic information hitherto obtainable only by the methods of atomic or molecular beams.

[1)]Within the framework of second-order perturbation theory, a spike at the frequency $\Omega_\mu = k_\mu\Omega/k$ corresponds to a two-quantum m-g transition [30]. The minimum width of the spike is reached when the Doppler shifts are cancelled out ($k_\mu \approx k$) and turns out to be equal to the arithmetic mean of the level widths.

[1] C. Townes and A. Schawlow, Microwave Spectroscopy, McGraw-Hill, 1955.
[2] E. B. Aleksandrov, A. M. Bonch-Bruevich, N. N. Kostin, and V. A. Khodovoĭ, ZhETF Pis. Red. 3, 85 (1966) [JETP Lett. 3, 53 (1966)].
[3] A. M. Bonch-Bruevich and V. A. Khodovoĭ, in: Nelineĭnaya optika (Nonlinear Optics), Nauka, SO, 1968.
[4] A. M. Bonch-Bruevich and V. A. Khodovoĭ, Usp. Fiz. Nauk 93, 71 (1967) [Sov. Phys.-Usp. 10, 637 (1967)].
[5] A. M. Bonch-Bruevich, N. N. Kostin, V. A. Khodovoĭ, and V. V. Khromov, Zh. Eksp. Teor. Fiz. 56, 144 (1969) [Sov. Phys.-JETP 29, 82 (1969)].
[6] P. A. Apanasevich, Deĭstvie lazernogo izlucheniya na veshchestvo, (Effects of Laser Radiation on Matter), Nauka i Tekhnika, 1973.
[7] Yu. M. Kirin, D. P. Kovalev, S. G. Rautian, and R. I. Sokolovskiĭ, ZhETF Pis. Red. 9, 7 (1969) [JETP Lett. 9, 3 (1969)].
[8] R. Bennett, Jr., Phys. Rev. 126, 580 (1962).
[9] S. G. Rautian, Tr. FIAN SSSR 43, 3 (1968).
[10] R. Karplus and J. Schwinger, Phys. Rev. 73, 1020 (1948).
[11] A. M. Bonch-Bruevich, and V. A. Khodovoĭ, Usp. Fiz. Nauk 85, 3 (1965) [Sov. Phys.-Usp. 8, 1 (1965)].
[12] L. D. Landau and E. M. Lifshitz, Kvantovaya mekhanika (Quantum Mechanics), Fizmatgiz, 1968, Sec. 40.
[13] V. B. Berestetskiĭ, E. M. Lifshitz, and L. P. Pitaevskiĭ, Relyativistskaya kvantovaya teoriya (Relativistic Quantum Theory), Chap. 1, Nauka, 1968.
[14] V. A. Fock and A. V. Tulub, Vestn. LGU, No. 16, 7 (1965).
[15] S. G. Rautian and I. I. Sobel'man, Zh. Eksp. Teor. Fiz. 41, 456 (1961) [Sov. Phys.-JETP 14, 328 (1962)].
[16] P. A. Dirac, Principles of Quantum Mechanics, Oxford, 1958.
[17] L. D. Zusman and A. I. Burshteĭn, Zh. Eksp. Teor. Fiz. 61, 976 (1971) [Sov. Phys.-JETP 34, 520 (1972)].
[18] S. G. Przhibel'skiĭ and V. A. Khodovoĭ, in: Nelineĭnye protsessy v optike (Nonlinear Processes in Optics), No. 2, Nauka, SO, 1972.
[19] P. A. Apanasevich, Zh. Prikl. Spektrosk. 12, 231 (1970).
[20] R. I. Sokolovskiĭ, Opt. Spektrosk. 28, 1033 (1970).
[21] T. Hänsch and P. Toschek, Proc. of the Conference on Laser and Opto-electronics (Southampton, March 1969), L., IERE, 1969.
[22] T. Hänsch, R. Kell, A. Schabert, Ch. Schmelzer, and P. Toschek, Zs. Phys. 226, 293 (1969).
[23] A. K. Popov, Zh. Eksp. Teor. Fiz. 58, 1623 (1970) [Sov. Phys.-JETP 31, 870 (1970)].
[24] E. B. Aleksandrov, Opt. Spektrosk. 14, 436 (1963).
[25] E. B. Aleksandrov and V. P. Kozlov, ibid. 16, 533, 1068 (1964).
[26] P. I. Sokolovskiĭ, ibid. 26, 870 (1969).
[27] M. S. Feld and A. Javan, Phys. Rev. 177, 450 (1969).
[28] T. Ya. Popova, A. K. Popov, S. G. Rautian, and R. I. Sokolovskiĭ, Zh. Eksp. Teor. Fiz. 57, 850 (1969) [Sov. Phys.-JETP 30, 466 (1970)].
[29] G. E. Notkin, S. G. Rautian, and A. A. Feoktistov, ibid. 52, 1673 (1967) [25, 1112 (1967)].
[30] H. K. Holt, Phys. Rev. Lett. 19, 1275 (1967); 20, 410 (1968).
[31] T. Ya. Popova, A. K. Popov, S. G. Rautian, and A. A. Feoktistov, Zh. Eksp. Teor. Fiz. 57, 444 (1969) [Sov. Phys.-JETP 30, 243 (1970)].
[32] I. L. Fabelinskiĭ, Molekulyarnoe rasseyanie sveta (Molecular Scattering of Light), Nauka, 1965.
[33] S. G. Rautian and A. A. Feoktistov, Zh. Eksp. Teor. Fiz. 56, 227 (1969) [Sov. Phys.-JETP 29, 126 (1969)].
[34] A. A. Feoktistov, Candidate's dissertation, FIAN SSSR (1969).
[35] F. A. Vorob'ev and R. I. Sokolovskiĭ, Zh. Prikl. Spektrosk. 13, 66 (1970).
[36] B. J. Feldman and M. S. Feld, Phys. Rev. A5, 899 (1972).
[37] T. Hänsch and P. Toschek, Zs. Phys. 236, 213 (1970).
[38] I. M. Beterov, Yu. A. Matyugin, and V. P. Chebotaev, IFP SO Akad. Nauk SSSR Preprint No. 21, Novosibirsk, 1971.
[39] A. Javan, In: "Quantum Optics and Electronics", N. Y., Gordon and Breach, 1965, p. 383.
[40] J. A. White, J. Opt. Soc. Am. 55, 1436 (1965).
[41] W. R. Bennett, Jr., V. P. Chebotayev, and J. W. Knutson, 5th Intern. Conference on Physics of Electron and Atomic Collisions. Abstract of Papers, L., Nauka, 1967.
[42] R. H. Cordover, P. A. Bonczyk, and A. Javan, Phys. Rev. Lett. 18, 730 (1967).
[43] W. G. Schweitzer, M. M. Birky, and J. A. White, J. Opt. Soc. Am. 57, 1226 (1967).
[44] I. M. Beterov and V. P. Chebotaev, ZhETF Pis. Red. 9, 216 (1969) [JETP Lett. 9, 127 (1969)].
[45] I. M. Beterov, Candidate's Dissertation, SO Akad. Nauk SSSR, Novosibirsk, 1970.
[46] N. G. Basov and V. S. Letokhov, FIAN SSSR Preprint No. 80, Moscow, 1969.
[47] V. P. Chebotayev, I. M. Beterov, and V. N. Licitsyn, IEEE J. Quantum Electron. QE-4, 389, 788 (1968).
[48] T. Hänsch and P. Toschek, ibid., p. 467; QE-5, 61 (1969).
[49] P. W. Smith, ibid. QE-1, 343 (1965).
[50] S. N. Atutov, V. S. Kuznetsov, S. G. Rautian, É. G. Saprykin, and R. N. Yudin, Tezisy dokladov na Vsesoyuznom simpoziume po fizike gazovykh OKG (Abstracts of Papers at All-Union Symposium on Gas-Laser Physics), Novosibirsk, 1969.
[51] I. M. Beterov, Yu. A. Matyugin, and V. P. Chebotaev, ZhETF Pis. Red. 10, 296 (1969) [JETP Lett. 10, 187 (1969)].
[52] I. M. Beterov, Yu. A. Matyugin, and V. P. Chebotaev, ibid. 12, 174 (1970) [12, 120 (1970)].
[53] I. M. Beterov, Yu. A. Matyugin, and V. P. Chebotaev, Opt. Spektrosk. 28, 357 (1970); I. M. Beterov, Yu. A. Matyugin, S. G. Rautian, and V. P. Chebotaev, Zh. Eksp. Teor. Fiz. 58, 1243 (1970) [Sov. Phys.-JETP 31, 668 (1970)].
[54] T. W. Ducas, M. S. Feld, L. W. Ryan, Jr., N. Skribanowitz, and A. Javan, Phys. Rev. A5, 1036 (1972).

Translated by J. G. Adashko